



# Deriving daily evapotranspiration from remotely sensed instantaneous evaporative fraction over olive orchard in semi-arid Morocco

Joost Hoedjes, Ghani Chehbouni, Frédéric Jacob, J. Ezzahar, Gilles Boulet

## ► To cite this version:

Joost Hoedjes, Ghani Chehbouni, Frédéric Jacob, J. Ezzahar, Gilles Boulet. Deriving daily evapotranspiration from remotely sensed instantaneous evaporative fraction over olive orchard in semi-arid Morocco. *Journal of Hydrology*, 2008, 254 (1-4), pp.53-64. 10.1016/j.jhydrol.2008.02.016 . ird-00388433

**HAL Id: ird-00388433**

**<https://hal.ird.fr/ird-00388433>**

Submitted on 28 May 2009

**HAL** is a multi-disciplinary open access archive for the deposit and dissemination of scientific research documents, whether they are published or not. The documents may come from teaching and research institutions in France or abroad, or from public or private research centers.

L'archive ouverte pluridisciplinaire **HAL**, est destinée au dépôt et à la diffusion de documents scientifiques de niveau recherche, publiés ou non, émanant des établissements d'enseignement et de recherche français ou étrangers, des laboratoires publics ou privés.



available at [www.sciencedirect.com](http://www.sciencedirect.com)



journal homepage: [www.elsevier.com/locate/jhydrol](http://www.elsevier.com/locate/jhydrol)



# Deriving daily evapotranspiration from remotely sensed instantaneous evaporative fraction over olive orchard in semi-arid Morocco

J.C.B. Hoedjes <sup>a</sup>, A. Chehbouni <sup>a,\*</sup>, F. Jacob <sup>b</sup>, J. Ezzahar <sup>c</sup>, G. Boulet <sup>a</sup>

<sup>a</sup> IRD/CESBIO, UMR: CNES-CNRS-UPS-IRD, 18 Avenue Edouard Belin, 31401 Toulouse Cedex 9, France

<sup>b</sup> IRD, UMR LISAH, 2 Place Viala, 34060 Montpellier, France

<sup>c</sup> University Cadi-Ayyad, Marrakech, Morocco

Received 7 August 2007; received in revised form 21 January 2008; accepted 24 February 2008

## KEYWORDS

Evapotranspiration;  
Evaporative fraction;  
Diurnal course;  
Available energy;  
ASTER;  
Semi-arid regions;  
Olive orchard

**Summary** Hydrology and crop water management require daily values of evapotranspiration ET at different time-space scale. Sun synchronous optical remote sensing, which allows for the assessment of ET with high to moderate spatial resolution, provides instantaneous estimates during satellites overpass. Then, usual solutions consist of extrapolating instantaneous to daily values by assuming that evaporative fraction EF is constant throughout the day, providing that daily available energy AE is known. The current study aims at deriving daily ET values from ASTER derived instantaneous estimates, over an olive orchard in a semi-arid region of Moroccan. It has been shown that EF is almost constant under dry conditions, but it depicts a pronounced concave up shape under wet conditions. A new heuristic parameterization is then proposed, which is based on the combination of routine daily meteorological data for characterizing atmospheric dependence, and on optical remote sensing based estimates of instantaneous EF values to take into account the dependence on soil and vegetation conditions. Using the same type of approach, a similar parameterization is next developed for AE. The validation of both approaches shows good performances. The overall method is finally applied to ASTER data. Though performances are reasonably good, their moderate reduction is ascribed to errors on remotely sensed variables. Future works will focus on method portability since its empirical formulation does not account for the direct stomatal response to water availability, as well as on application over different surface and climate conditions.

© 2008 Published by Elsevier B.V.

\* Corresponding author. Tel.: +33 (0)5 61 55 8197; fax: +33 (0)5 61 55 85 00.

E-mail addresses: [joost.hoedjes@cesbio.cnes.fr](mailto:joost.hoedjes@cesbio.cnes.fr) (J.C.B. Hoedjes), [ghani@cesbio.cnes.fr](mailto:ghani@cesbio.cnes.fr) (A. Chehbouni), [frederic.jacob@supagro.inra.fr](mailto:frederic.jacob@supagro.inra.fr) (F. Jacob), [j.ezzahar@ucam.ac.ma](mailto:j.ezzahar@ucam.ac.ma) (J. Ezzahar), [gilles.boulet@cesbio.cnes.fr](mailto:gilles.boulet@cesbio.cnes.fr) (G. Boulet).

## Introduction

Estimates of regional evapotranspiration (ET) are of crucial need for climate studies, weather forecasts, hydrological surveys, ecological monitoring, and water resource management (Van den Hurk et al., 1997; Su, 2000; Bastiaanssen et al., 2000). Given that distributed hydrological models can accurately estimate basin scale runoff while poorly reproducing other hydrological cycle components, intermediate processes such as soil moisture and thus ET have to be well simulated (Chaponnière et al., 2007). Within semiarid agricultural regions, which hydrological cycle is strongly influenced by ET through crop water consumption, a precise ET estimation is of importance for water saving through efficient irrigation practices (Allen, 2000; Ohmura and Wild, 2002; Porporato et al., 2004; Wild et al., 2004). Among the several research programs designed to develop efficient irrigation management tools in arid and semi-arid zones, the SUDMED (Chehbouni et al., in press-a) and IRRIMED (<http://www.irimed.org>) projects have taken place in southern Mediterranean regions, to assess the spatio-temporal variability of water needs and consumption for irrigated crops under water limited conditions.

Optical satellite remote sensing is a promising technique for estimating instantaneous and daily ET at global and regional scale, via surface energy budget closure. The methods proposed in the literature range from simple and empirical approaches, to complex and data consuming ones (Glenn et al., 2007). Among the complex methods are Soil Vegetation Atmosphere Transfer (SVAT) models, which describe the diurnal course of heat and mass transfers, provided micrometeorological conditions and water/energy balance parameters are documented (Braud et al., 1995; Mahfouf et al., 1995; Olioso et al., 1996; Calvet et al., 1998; Olioso et al., 2005; Coudert et al., 2006; Gentine et al., 2007). Among the simple approaches are the simplified relationship, which links daily ET to midday near surface temperature gradient (Jackson et al., 1977). In the same vein, the FAO-56 method expresses daily ET using crop coefficients derived from vegetation indexes, but needs to be calibrated with ground measurements (Duchemin et al., 2006; Er-Raki et al., 2007a, Yang et al., 2006). Between complex and empirical approaches, compromising solutions are energy balance models. They compute at satellite overpass instantaneous ET as the residual term of energy budget, once net radiation, soil heat flux and sensible heat flux are derived (Bastiaanssen et al., 1998; Norman et al., 2003; Su, 2002; Caparrini et al., 2003, 2004; French et al., 2005; Crow and Kustas, 2005; Allen et al., 2007; Cleugh et al., 2007; Mu et al., 2007).

Instantaneous values of ET at satellite overpass can be used as diagnostics for surface status (Chandrapala and Wimalasuriya, 2003), or as controls for hydrological models through assimilation schemes (Schuurmans et al., 2003). However, their interest in terms of water management is limited, since the latter requires daily values (Bastiaanssen et al., 2000). Daily ET can be derived from FAO-56 or simplified relationship, but difficulties arise when extrapolating outside the environmental conditions considered for calibration. The ET diurnal course can be inferred assimilating sun synchronous observations into SVAT models, but this is

limited by uncertainties when estimating SVAT parameters and initial variables. The ET diurnal course can also be retrieved using geostationary observations, but the kilometeric resolutions severely limit water management at the field scale. Probably, the most practical solution is estimating instantaneous values from energy balance models combined with sun synchronous observations, and next extrapolating at the daily scale by presuming generic trends for the diurnal courses of ET and related variables.

Assuming generic trend for the ET diurnal course can consist of approximating the latter by a sine function, given it is similar to that of solar irradiance. However, this method is limited by its empirical character in terms of accuracy (Zhang and Lemeur, 1995). Another possibility is assuming a typical shape for Evaporative Fraction (EF) given Available Energy (AE) is known. The EF is defined as the ratio of ET to AE, and AE is the difference between net radiation and soil heat flux. EF is in deed an important indicator of the surface hydrological history, including wetting and drying events (Shuttleworth et al., 1989; Nichols and Cuenca, 1993). Thus, it was suggested to assume a constant daytime EF, to be used with daily AE for deriving daily ET (Sugita and Brutsaert, 1991; Roerink et al., 2000; Gomez et al., 2005).

Assuming a daytime constant EF is not straightforward, regarding what has been reported from both theoretical and experimental based investigations (Crago, 1996; Crago and Brutsaert, 1996). Zhang and Lemeur (1995) observed EF changes with environmental variables, especially AE and surface resistance. Suleiman and Crago (2004) reported that EF increases with vegetation amount, soil moisture and air dryness. Baldocchi et al. (2004) and Li et al. (2006) reported that stomatal conductance drives EF according to soil moisture since soil dryness tends to decrease both variables. During fair weather conditions over fully vegetated surfaces, Lhomme and Elguero (1999) reported from model simulation a typical concave-up shape for EF, quite constant during midday, and mainly driven by changes in soil moisture and solar energy. Thus, assuming a daytime constant EF equal to the noon value induces underestimations since this value is the lowest of the day. Finally, Gentine et al. (2007) showed that EF diurnal course mainly depends on both evaporative state and vegetation cover. Besides the EF diurnal course, addressing the daytime AE is a delicate issue. Empirical approaches have been proposed to derive it from instantaneous values, mainly approximating AE by a sine function (Jackson et al., 1983; Bastiaanssen et al., 2000). Again, the most adequate solution is using geostationary satellite observations, but the corresponding spatial resolutions make the use of such data complicated for water management at field scale.

In the same context of the investigations discussed above, the present study aims at inferring daily ET from sun synchronous optical remote sensing, with the objective of improving irrigation water management at the field scale. The challenge is then considering an irrigated old olive orchard in central Morocco, characterized by a semi-arid climate, tall trees, and strong soil moisture heterogeneity due to irrigation practices. This challenge was addressed in four steps. We first examine the EF diurnal behavior using Eddy Correlation (EC) measurements, and then quantify errors on daily ET when assuming EF self-preservation.

Second, we parameterize the EF diurnal course using a combination of routinely available meteorological data and a unique "one shot" instantaneous EF estimates. Third, we parameterize the AE diurnal cycle from ground based measurements of energy balance, also by considering routine micrometeorological measurements and a single instantaneous estimates of AE. Finally, the proposed parameterizations after being calibrated using ground based data are applied to ASTER data. These different steps are implemented using data collected during the 2003–2004 period. Given that ASTER data was only available in 2003, design and calibration were performed using ground-based 2004 dataset, while validation was performed using the 2003 one.

## Site description and experimental setup

The study took place in a semi-arid basin in central Morocco (the Tensift basin, Fig. 1) within the framework of the SUD-MED Program (<http://www.irrimed.org/sudmed>). In this section, site description and experimental setup are briefly summarized; the reader is referred to [Chehbouni et al. \(in press-a\)](#) for a complete description of both project and site. The regional climate was characterized by low and irregular rainfalls with a 240 mm annual average, an evaporative demand of about 1600 mm per year, and a dry atmosphere with a 56% average humidity. The experiment was carried out between Day Of Year (DOY) 288 in 2002 and DOY 271 in 2004, at the 275 ha Agdal olive orchard, southeastern of Marrakech (31°36'N, 07°58'W). The average height of the olive trees is 6.5 m, the average crown diameter is 6.5 m. The density of the olive trees at our site is about 225 ha<sup>-1</sup>. Understorey vegetation consists mainly of short weeds, with ground cover ranging from almost no (10–20%) cover to almost complete (70–80%) cover ([Hoedjes et al., 2007](#)). The olive trees are irrigated through level basin flood irrigation. For this purpose, each tree is surrounded by a small earthen levy, and water is directed to each tree through a network of ditches ([Williams et al., 2004](#)). On average, the irrigation takes approximately 12 days.

The experimental setup collected standard meteorological measurements: wind speed and direction (Young Wp200 anemometer); air temperature and humidity (Vaisala HMP45AC temperature and humidity probe). The instruments were set 9 m above ground (3 m above canopy).

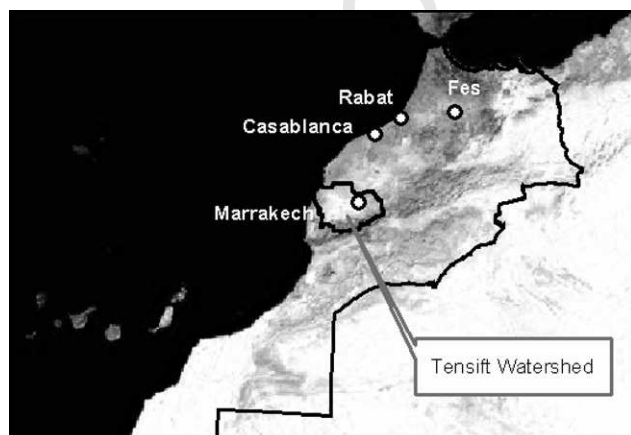


Figure 1 Location of the study area.

The four net radiation components were measured using a Kipp and Zonen CNR1 radiometer, set at an 8.5 m height to embrace vegetation and soil radiances by ensuring the field of view was representative of their respective cover fractions. Soil and vegetation brightness temperatures were measured using two Apogee IRTS-P. The soil heat flux density was measured using heat flux plates (HFT3-L, Campbell Scientific Ltd.) at three locations with contrasting amounts of radiation reaching the soil. The measurement depth was 1 cm. The plates were placed: one below the tree, near the trunk in order not to be exposed to direct solar radiation; one was exposed directly to solar radiation, the last one in an intermediate position. An average of these three measurements was made to obtain a representative value. Soil moisture and temperature were recorded at different depths within the 0–50 cm horizon, using CS616 water content reflectometer and TP107 temperature probes (both Campbell Scientific Ltd.), respectively. Measurements were sampled at 1 Hz, and 30 min averages were stored on CR10X dataloggers (Campbell Scientific Ltd.).

The EC system was installed at a 9.2 m height. During the first three months it included a CSAT 3 3D sonic anemometer (Campbell scientific Ltd.) and a LICOR-7500 open-path infrared gas analyzer (Campbell Scientific Ltd.). Raw data were sampled at a 20 Hz rate, recorded using a CR23X datalogger (Campbell scientific Ltd.). After three months, the LICOR-7500 was replaced by a KH20 Krypton hygrometer (Campbell Scientific Ltd.), and the CR23X was replaced with a CR5000 datalogger (Campbell Scientific Ltd.). The half-hourly fluxes were later calculated off-line using Eddy Covariance processing software 'ECPack', after performing all required corrections for planar fit correction, humidity and oxygen (KH20), frequency response for slow apparatus, and path length integration ([Van Dijk et al., 2004](#)).

The analysis showed that the sum of latent and sensible heat flux measured independently by the EC systems was often lower than available energy (AE). The absolute value of average closure was about 8% and 9% of available energy during the 2003 and 2004 seasons, respectively ([Er-Raki et al., 2007b](#)). This problem could not be explained neither by mismatching spatial extents for fluxes and AE measurements, nor by uncertainties associated with measurements of soil heat flux and net radiation ([Twine et al., 2000](#); [Hoedjes et al., 2002](#); [Chehbouni et al., in press-b, 2007c](#)). Correction was then performed using the approach suggested by [Twine et al. \(2000\)](#), which assumes the energy balance is due to underestimates from EC measurements while the corresponding Bowen ratio is correctly estimated. Based on this assumption, we re-computed sensible and latent heat fluxes by forcing the energy balance closure using the measured AE and Bowen ratio.

ASTER official products ([Abrams and Hook, 2002](#)) were downloaded from the Earth Observing System Data Gateway (EDG). Once instrumental effects are removed ([Fujisada, 1998](#); [Fujisada et al., 1998](#); [Abrams, 2000](#)), atmospheric corrections are performed using radiative transfer codes documented for atmospheric status ([Thome et al., 1998](#)), providing surface reflectance's over the solar domain (bands 1–9) and surface brightness temperatures over the thermal domain (bands 10–14). The latter are next used to derive surface emissivity and radiometric temperature by applying the Temperature Emissivity Separation algorithm ([Gillespie](#)



et al., 1998; Schmugge et al., 1998). Six ASTER images were collected over the study area, one in 2002 (DOY 311), and 5 in 2003 (DOY 58, 138, 202, 282 and 289). Spatial resolution is 15 m (respectively 30 m) for visible and near infrared (respectively shortwave) reflectance's, and 90 m for emissivity and radiometric temperature. Higher resolution products were linearly degraded to 90 m, given aggregation effects from spatial heterogeneities could be considered as minor over flat semiarid regions (Jacob et al., 2004; Liu et al., 2006).

## Method design, implementation and assessment

The parameterization is designed and assessed using ground based EC data collected during the 2003–2004 experimental period. ASTER data were only available in 2003. Therefore, design and calibration were performed using the 2004 dataset, whilst validation was performed using the 2003 ground and ASTER dataset. Furthermore, only daytime observations from 09:30 to 16:30 UTC are considered, since the most important latent heat fluxes occur during this period.

### EF diurnal course and impact-assessment on ET estimates

In this section we assess the validity of EF self-preservation using the EC data during dry and wet conditions. It is important to mention that dry or wet conditions should normally be characterized by soil moisture conditions. However, since we are dealing with the EF which is influenced by both surface and atmospheric conditions, we preferred instead to use the Bowen Ratio ( $BR = H/LE$ ) with a threshold value higher (lower) than 1.5 as indicator of dry (wet) conditions. Fig. 2a displays the observed diurnal variations of EF as well as the EF constant value set up to that observed at 11:30 UTC (ASTER time overpass) for 10 cloud free days under dry conditions, selected between DOY 80 and DOY 221 in 2004. The same curves are presented in Fig. 2b, for a 10-day cloud free period in 2004 under wet conditions. It can be seen that that assuming EF self-preservation is valid under dry conditions, since EF is relatively constant despite

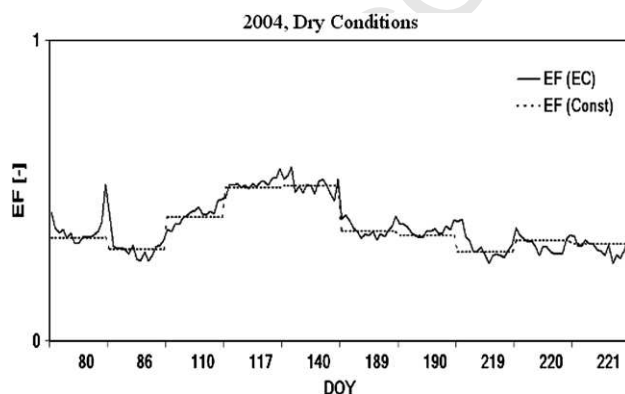


**Figure 2a** Eddy Covariance (EC) derived evaporative fraction EF (EC) and constant EF (at 11:30) for 10 selected dry and cloud free days within the 2004 selected between DOY 80 and DOY 221.

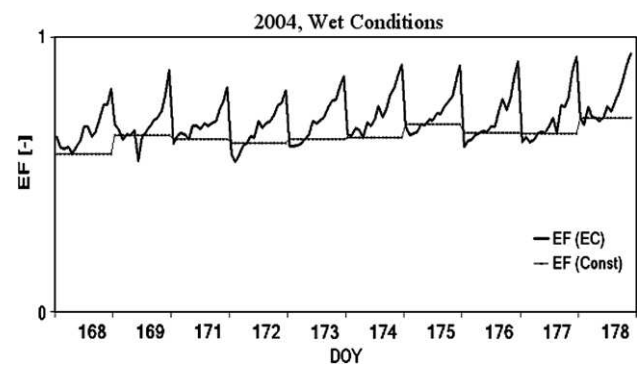


**Figure 2b** The same as Fig. 2a for 10 wet days following an irrigation event in 2004 (DOY 168–178).

observed some daily variation. But this assumption is not valid under wet conditions, since EF depicts a concave-up shape with a straight decrease in early morning and a sharp increase in late afternoon. Thus, assuming EF is constant and equal to EF @ 11:30 UTC underestimates actual daytime EF and consequently latent heat flux. These results corroborate those reported by Lhomme and Elguero (1999), Suleiman and Crago (2004) and Gentine et al. (2007).

Next, we quantify the errors on daytime ET when assuming a constant EF. The ET diurnal course is estimated combining a daily constant EF and in situ data of AE:

$$ET_{EF, const} = EF^{1130} AE = EF^{1130} (R_n - G) \quad (1)$$

Fig. 3a and b displays comparisons of half hourly ET values simulated from Eq. (1) against observations for dry and wet conditions in 2004, respectively. As it might be expected, assuming EF self-preservation appears to be valid under dry conditions, with an RMSE between observed and simulated ET of  $14 \text{ W m}^{-2}$  (calibration residual error) and a Nash–Sutcliffe coefficient of 0.94. Under wet conditions, however, assuming a constant EF significantly underestimates ET, with an RMSE between observations and simulations of  $46 \text{ W m}^{-2}$ , and a Nash–Sutcliffe coefficient of

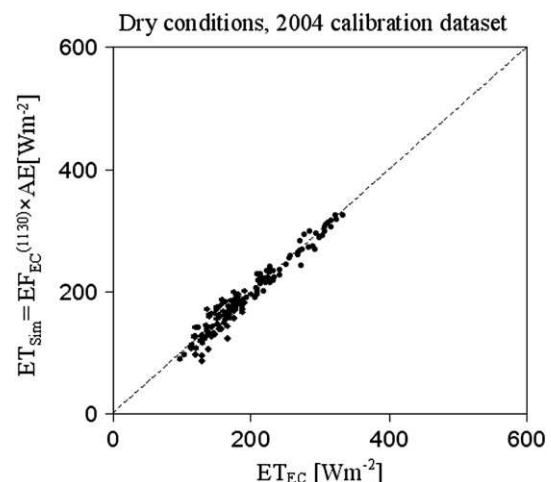


**Figure 3a** Comparison between eddy covariance latent heat flux ( $ET_{EC}$ ) and latent heat flux calculated using  $EF_{EC}$  at 11:30 as constant during daytime ( $ET_{sim}$ ) during the 10 dry days in 2004.

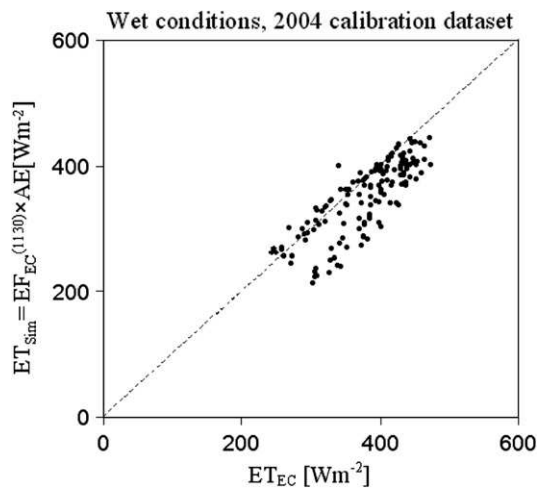


**Figure 3b** Comparison between eddy covariance latent heat flux ( $ET_{EC}$ ) and latent heat flux calculated using  $EF_{EC}$  at 11:30 as constant during daytime ( $ET_{Sim}$ ) during a 10-day period following an irrigation event in 2004.

0.34. Thus, the validity of assuming EF self-preservation depends on soil moisture. It is therefore necessary under wet condition to account for the diurnal cycle of EF to derive accurate estimates of daytime ET.

### Parameterizing the EF diurnal cycle

An alternative to assuming EF self preservation is proposed here, through a heuristic approach that parameterizes the EF diurnal cycle. The constraints are accounting for the EF daytime relative stability under dry conditions, and adequately reproducing the EF diurnal course during wet conditions. For operational applications at the irrigation district scale, the dependence must rely on routinely measured parameters which remain reasonably constant at such scale, or on parameters available from remote sensing. Given the EF diurnal cycle depends on both atmospheric forcing and surface conditions (Gentine et al., 2007), parameterizing the diurnal behavior of EF is twofold. First, the diurnal cycles of atmospheric forcing are considered, since atmospheric demand is controlled by incoming radiation, relative humidity and, to a lesser extent, wind speed. Second, we account for land surface heterogeneities potentially available from remotely sensed thermal data, since control on surface temperature is exerted by vegetation characteristics and most importantly by soil moisture status.

Since an increase in EF mainly results from an increase in incoming solar radiation and a decrease in atmospheric humidity (Lhomme and Elguero, 1999; Suleiman and Crago, 2004; Gentine et al., 2007), the first step consists of parameterizing the diurnal shape of EF as a function of the main atmospheric forcing parameters, i.e. incoming solar radiation  $S^{\downarrow}$  and relative humidity RH. The proposed parameterization reads:

$$EF_{Sim} = 1.2 - (0.4 \frac{S^{\downarrow}}{1000} + 0.5 \frac{RH}{100}) \quad (2)$$

Though Eq. (2) provides a good representation of the relative EF diurnal course, the magnitude and the day-to-day variation of the EF absolute minimum depend on soil moisture conditions. Therefore, the second step aims at incorporating, a daily scaling factor in order to produce the actual day to day variation of EF ( $EF_{Sim}^{ACT}$ ). In order to use efficiently remote sensing data, this scaling factor  $r_{EF}^{1130}$  is expressed as the ratio of simulated to actual EF when ASTER overpasses @ 11:30 UTC:

$$EF_{Sim}^{ACT} = EF_{Sim} r_{EF}^{1130} \quad (3)$$

with

$$r_{EF}^{1130} = \frac{EF_{Obs}^{1130}}{EF_{Sim}^{1130}} \quad (4)$$

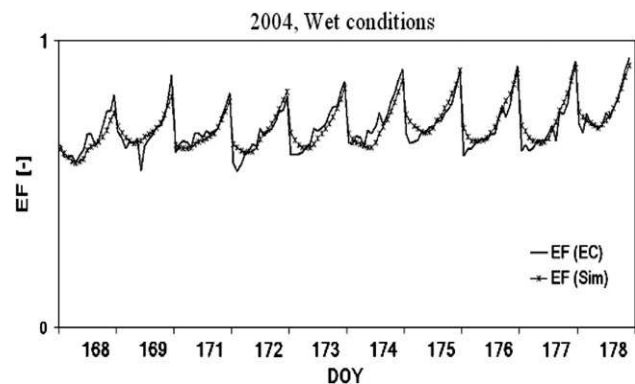
For development purposes,  $EF_{Obs}^{1130}$  is obtained from EC latent heat observations as well as locally measured AE @ 11:30 UTC, and is written as  $EF_{EC}^{1130}$ . Later on,  $EF_{Obs}^{1130}$  will be derived from remote sensing data only, using ASTER data to derive latent heat, and routinely available data to estimate AE; it will be named  $EF_{ASTER}^{1130}$ .

To account for the validity of EF self preservation under dry conditions which usually corresponds to Bower ratio values higher than 1.5, the complete EF parameterization becomes:

$$EF_{Sim}^{ACT} = \begin{cases} EF_{Sim} r_{EF}^{1130} & \beta^{1130} \leq 1.5 \\ EF_{Obs}^{1130} & \beta^{1130} > 1.5 \end{cases} \quad \text{for} \quad \beta^{1130} \leq 1.5 \quad (5)$$

To assess the performance of this proposed parametrization, we present in Fig. 4 chronicles of measured (EF<sub>EC</sub>) and simulated (EF<sub>Sim</sub>) EF, for the same 10-day period than Fig. 2b (2004, wet conditions). Compared to the constant daytime EF as provided in Fig. 2b, EF<sub>Sim</sub> approximates in a better way the observed EF diurnal variation (EF<sub>EC</sub>). In order to evaluate the resulting improvement in terms of evaporation estimates, latent heat flux is derived from parameterized EF and in situ observations of AE during the day:

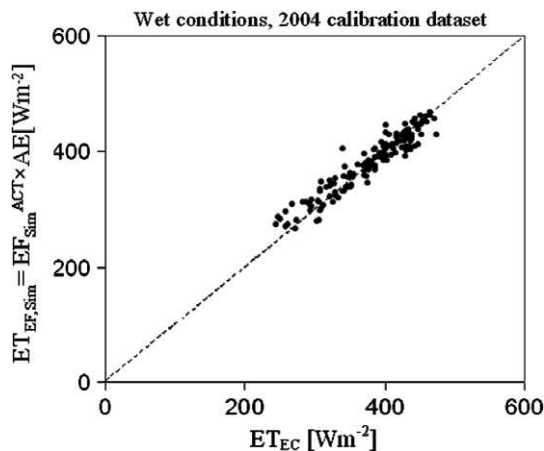
$$ET_{EF,Sim} = EF_{Sim}^{ACT} (R_n - G) \quad (6)$$



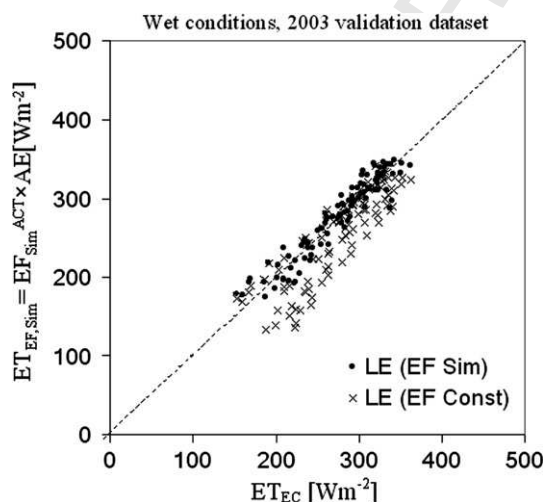
**Figure 4** Comparison between time course of eddy correlation based EF values and those simulated using the parameterization given in Eqs. (2)–(4) for 10 days period under wet conditions in 2004 season.

Fig. 5 presents a comparison between measured ET values and those simulated using Eq. (6) over the 10-day wet period in 2004. It can be clearly seen that taking into account the diurnal variation of EF significantly improves ET retrieval. RMSE between measured and simulated ET values was of  $18 \text{ W m}^{-2}$  and a Nash–Sutcliffe coefficient of 0.9, as compared to  $46 \text{ W m}^{-2}$  and 0.34, respectively when using a constant EF.

In order to extend this evaluation with independent dataset, a 10-day periods (wet conditions) during 2003 were selected. Fig. 6 shows the comparison between  $ET_{EF,Sim}$  and  $ET_{EC}$  including ET estimates when assuming a constant EF. It is shown that the proposed parameterization for EF adequately retrieves the observed values of ET compared to assuming a constant EF during the day. Indeed, RMSE value is about  $15 \text{ W m}^{-2}$  and the Nash–Sutcliffe coefficient is 0.90. Finally, the interest of the proposed EF parameterization for water balance studies is assessed in terms of



**Figure 5** Comparison between measured ET values ( $ET_{EC}$ ) and those simulated using Eq. (6) for the same 10-days period under wet conditions in 2004 season.



**Figure 6** Comparison between  $ET_{EC}$  and  $ET_{Sim}$  during wet conditions in 2003.  $ET_{Sim}$  is calculated both using the proposed parameterization (dots) and, for illustration, using  $EF_{EC}$  at 11:30 as constant daytime value (crosses).

**Table 1** Water lost through evapotranspiration during two 10-day wet periods (2004 and 2003, daytime values only); measured, simulated with constant EF and simulated with variable EF

Method	Measured (EC) [mm]	Simulated, Constant EF [mm]	Simulated, Variable EF [mm]
2004	41.3	38.1	41.3
2003	20.9	19.3	21.0

water losses through evapotranspiration during the two wet periods in 2003 and 2004 (Table 1). In both cases, it is shown using a daytime constant EF for the calculation of ET underestimated the amount of water lost through evapotranspiration by 8%. Conversely, using the proposed EF parameterization in the calculation of ET reduces the error on water loss to less than 0.5%.

### Parameterizing the AE diurnal course

Implementing Eq. (6) for ET calculation requires the diurnal course of  $AE = R_n - G$ , which is not routinely available. Various formulations were proposed for estimating AE at a given time of the day (Jackson et al., 1983; Seguin et al., 1989; Bastiaanssen et al., 2000), usually based on sine functions and thus not accounting for any atmospheric disturbance (e.g. Bisht et al., 2005). Another solution is using instantaneous remote sensing observations when ASTER overpasses (11:30 UTC), and then extrapolating the AE diurnal course from parameterizations based on meteorological measurements that remain fairly constant at the scale of the irrigation district. As for the EF parameterization, a heuristic approach is used for the AE diurnal course, by considering surface net radiation without thermal emission component:

$$\left( \frac{(R_n - G)^t}{(R_n - G)_{Obs}^{1130}} \right) = f \left( \frac{R^{*t}}{R^{*1130}} \right) \quad (7)$$

where  $R^{*t}$  is a function of solar irradiance ( $S^\downarrow$ ) and atmospheric thermal irradiance ( $L^\downarrow$ ):

$$R^{*t} = (1 - \alpha) S^\downarrow + \varepsilon L^\downarrow \quad (8)$$

with  $\alpha$  and  $\varepsilon$  surface albedo and emissivity, respectively. They are available from remote sensing and are considered relatively constant throughout the day.  $S^\downarrow$  is available from meteorological networks or geostationary remote sensors, and  $L^\downarrow$  can be derived from air temperature and humidity (Brutsaert, 1982). Assuming albedo is constant throughout the day can be far from reality (Jacob and Oliosio, 2005), but the validation exercise reported below shows this is not critical for accurately retrieving the AE diurnal course. The 2nd order function  $f$  is expressed as:

$$f \left( \frac{R^{*t}}{R^{*1130}} \right) = a_2 \left( \frac{R^{*t}}{R^{*1130}} \right)^2 + a_1 \left( \frac{R^{*t}}{R^{*1130}} \right) + a_0 \quad (9)$$

Calibrating Eq. (9) over the EC 2004 dataset provided for the coefficients:  $a_2 = 0.34285$ ;  $a_1 = 1.15120$ ;  $a_0 = -0.48495$ . By incorporating Eqs. (8) and (9) into Eq. (7); half hourly AE



values are obtained using only diurnal measurements of  $S^{\downarrow}$ ,  $L^{\downarrow}$ , and the single observation  $R_n - G_{Obs}^{130}$  when ASTER overpasses. Fig. 7a and b displays the comparison between observed and parameterized AE over the two years (2004 for calibration and 2003 for validation), respectively. For both cases, it is shown the proposed parameterization is adequate, with RMSE values ranging from 22  $W m^{-2}$  for the calibration dataset to 30  $W m^{-2}$  for the validation dataset.

## Application to ASTER data

The proposed parameterizations for the AE and EF diurnal courses rely on standard meteorological data for characterizing the daytime variations, and on remotely sensed observations to account for surface heterogeneities induced by differences in soil moisture and vegetation. Given land surface conditions hardly change throughout the day, and cloud free meteorological conditions are almost homogeneous over the study area, the simulated AE, EF and ET can be considered as representative. It is thus relevant

applying this approach to ASTER observations, which 90 m spatial resolution for thermal imagery is amongst the finest possibilities and reduces problems due to mixed pixels (French et al., 2005). Under unstable conditions, an ASTER pixel footprint is larger than the source area for a typical EC system. However, this source area is often located within adjacent ASTER pixels. A footprint analysis is therefore necessary before any comparison between remote sensing and in situ observations. To compute the contribution of each part of the source area (i.e. the footprint of the flux measurement), several approaches have been developed over the last decades. These range from simple analytical models (e.g. Schuepp et al., 1990) to complex Lagrangian models (e.g. Baldocchi, 1997; Rannik et al., 2000) or models based on large eddy simulations (e.g. Leclerc et al., 1997). As compared to analytical models, the complex models provide more realistic footprint simulations over forest canopies, and they can account for inhomogeneous turbulence. However, they require significantly larger computational power. Despite the lack of complexity, Finn et al. (1996) reported the analytical model proposed by Horst and Weil (1992, 1994) produces very similar results to a Lagrangian stochastic model, and can therefore be considered as a reliable method. We therefore select this model, which is fully described over the same study site in Hoedjes et al., 2007.

## Obtaining fluxes from ASTER observations

Calculating land surface net radiation and soil heat flux requires apparent albedo (Jacob and Olioso, 2005), broadband emissivity over the [3–100]  $\mu m$  spectral range, and vegetation cover. Albedo (respectively emissivity) is calculated as a linear combination of visible and near infrared reflectance (respectively thermal infrared emissivities), following Jacob et al. (2002) (respectively Ogawa et al. (2003)) for the weighting coefficients. Vegetation cover is computed from Normalized Difference Vegetation Index using the empirical relationship proposed by Asrar et al. (1984), and following Weiss et al., 2002 for implementation. Then, net radiation ( $R_n^{ASTER}$ ) is classically inferred using ASTER derived albedo, broadband emissivity, and surface radiometric temperature, along with field observations for solar and thermal irradiances. The ratio of soil heat flux ( $G^{ASTER}$ ) to net radiation is calculated according to Santanello and Friedl (2003). Using radiative surface temperature inferred from ASTER imagery, the semi-empirical model proposed by Lhomme et al. (1994) is used to obtain sensible heat flux:

$$H^{ASTER} = \rho c_p \left[ \frac{(T_r^{ASTER} - T_a) - c \delta T}{r_a - r_e} \right] \quad (10)$$

where  $c_p$  is specific heat of air at constant pressure,  $\rho$  is air density,  $T_a$  is potential air temperature at reference height (K) and  $r_a$  is aerodynamic resistance to heat transfer between the canopy source and the reference height (Brutsaert, 1982). Equivalent resistance  $r_e$  is given by:

$$r_e = \frac{r_{af} r_{as}}{(r_{af} + r_{as})} \quad (11)$$

where  $r_{as}$  is aerodynamic resistance between the soil and the canopy source height (Shuttleworth and Gurney, 1990), and  $r_{af}$  is canopy bulk boundary layer resistance

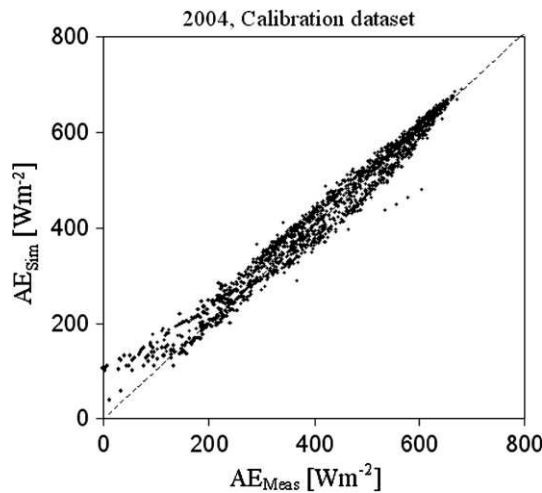


**Figure 7a** Measured vs. simulated available energy during the whole experimental period in 2004.

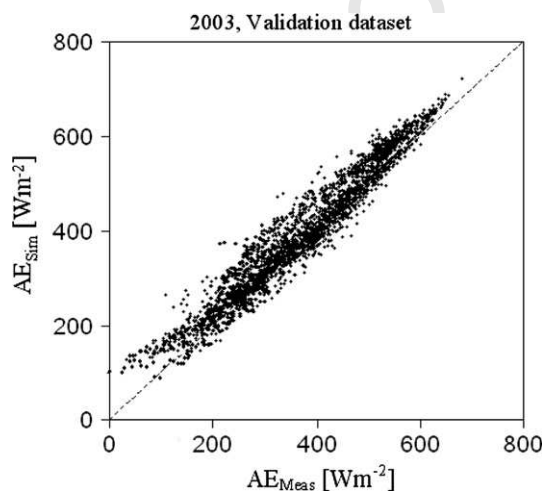


**Figure 7b** Validation of the AE parameterization for the 2003 experimental season.



(Choudhury and Monteith, 1988). This one source model is based on the bulk aerodynamic relationship, but benefits from a direct use of radiometric surface temperature, instead of aerodynamic surface temperature which is difficult to estimate (Jacob et al., in press). Furthermore, the temperature difference between the soil and the foliage is taken into account through the term ( $c\delta T$ ), which is given by:

$$\delta T = a(T_r^{\text{ASTER}} - T_a)^m \quad (12)$$

and

$$c = \left[ \frac{1}{1 + (r_{af}/r_{as})} \right] - f \quad (13)$$

Here  $f$  is the fractional vegetation cover,  $a$  and  $m$  are empirical coefficients ( $a = 0.25$  and  $m = 2$ ).

Using the footprint model, EC footprint weighted averages for  $R_n^{\text{ASTER}}$ ,  $G^{\text{ASTER}}$  and  $H^{\text{ASTER}}$  are calculated for each ASTER image acquisition. From these average values, the instantaneous EF, AE and Bowen ratio are estimated on ASTER overpass as

$$AE^{\text{ASTER}} = R_n^{\text{ASTER}} - G^{\text{ASTER}} \quad (14)$$

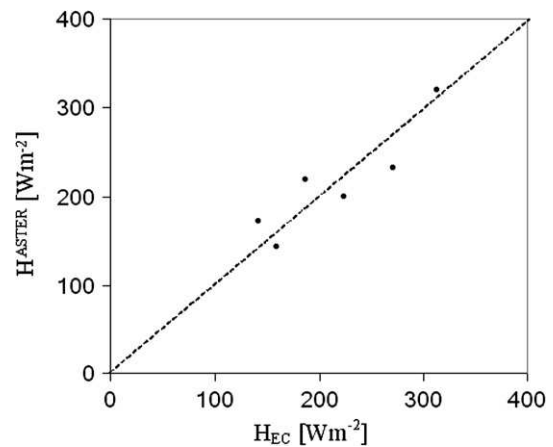
$$EF^{\text{ASTER}} = \frac{R_n^{\text{ASTER}} - G^{\text{ASTER}} - H^{\text{ASTER}}}{R_n^{\text{ASTER}} - G^{\text{ASTER}}} \quad (15)$$

$$\beta^{\text{ASTER}} = \frac{H^{\text{ASTER}}}{R_n^{\text{ASTER}} - G^{\text{ASTER}} - H^{\text{ASTER}}} \quad (16)$$

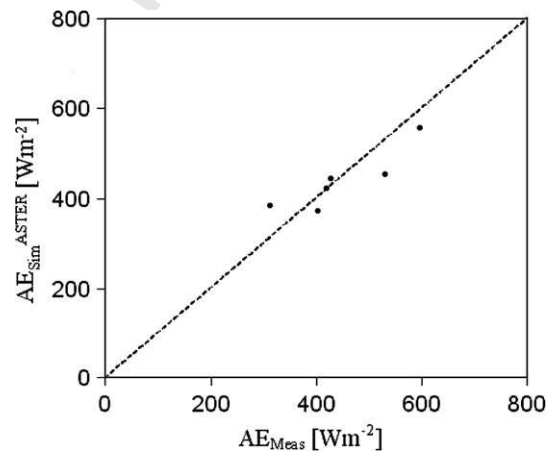
### Application of the methods

Fig. 8a and b displays the validation of  $H^{\text{ASTER}}$  against  $H_{\text{EC}}$  and of  $AE^{\text{ASTER}}$  against measured AE, for the 6 ASTER imagery acquisitions. The corresponding RMSE values between ground based and ASTER based estimates were  $27 \text{ W m}^{-2}$  for  $H$  and  $51 \text{ W m}^{-2}$  for AE. From these estimates, instantaneous EF and Bowen ratio are calculated using Eqs. (15) and (16). A comparison between  $EF^{\text{ASTER}}$  and  $EF_{\text{EC}}$  is shown in Fig. 9, the corresponding RMSE value being 0.06. Despite some scatter, results are comparable to those reported in earlier studies (Crow and Kustas, 2005; Batra et al., 2006; Wang et al., 2006). From the calculated Bowen ratio values, it is possible to examine occurrences of wet and dry conditions over the six days of ASTER imagery acquisition. Dry conditions were observed on one day, with  $\beta^{\text{ASTER}} > 1.5$ . On two days, wet conditions were due to irrigation events within one week before ASTER overpasses, with  $\beta^{\text{ASTER}}$  from 0.7 to 0.8. On three days, conditions were intermediate, with  $\beta^{\text{ASTER}}$  from 1.1 to 1.3.

Once inferred, instantaneous  $EF^{\text{ASTER}}$  is used in place of  $EF_{\text{Obs}}^{1130}$  in the parameterization scheme (Eqs. (3)–(5)), to obtain  $r_{\text{EF}}^{1130}$  and consequently the EF diurnal course  $EF_{\text{Sim}}^{\text{ASTER}}$ . Instantaneous  $AE^{\text{ASTER}}$  is used in Eq. (7) to calculate half-hourly values of  $AE_{\text{Sim}}^{\text{ASTER}}$ . Finally, the ET diurnal course  $ET_{\text{EF,Sim}}^{\text{ASTER}}$  is obtained from Eq. (6) using  $AE_{\text{Sim}}^{\text{ASTER}}$  and  $EF_{\text{Sim}}^{\text{ASTER}}$ . Fig. 10 displays the validation of  $ET_{\text{EF,Sim}}^{\text{ASTER}}$ . Linear regression yields  $ET_{\text{EF,Sim}}^{\text{ASTER}} = 0.77 ET_{\text{EC}} + 53$ , with  $R^2 = 0.63$  and  $\text{RMSE} = 48 \text{ W m}^{-2}$ . These moderate performances can result from 1/amplifications through the ET calculation of errors on remotely sensed variables, 2/assuming daytime albedo is constant which can be far from the reality (Jacob and Olioso, 2005), or 3/the error in  $H$  and AE simulations translates



**Figure 8a** Comparison between sensible heat fluxes obtained from the eddy covariance system and sensible heat fluxes calculated using the model proposed by Lhomme et al. (1994) combined with ASTER thermal imagery.



**Figure 8b** Comparison between measured available energy and that simulated using ASTER imagery.

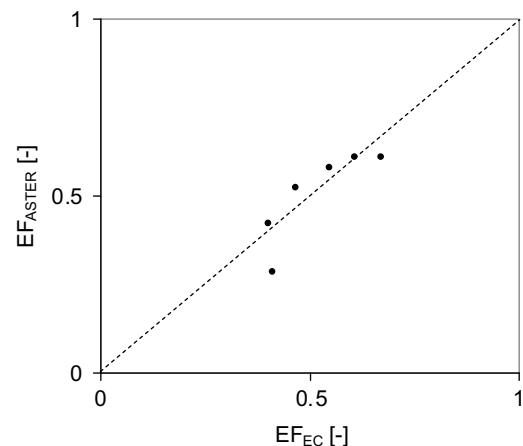


**Figure 9** Eddy covariance derived evaporative fraction compared to ASTER derived evaporative fraction.

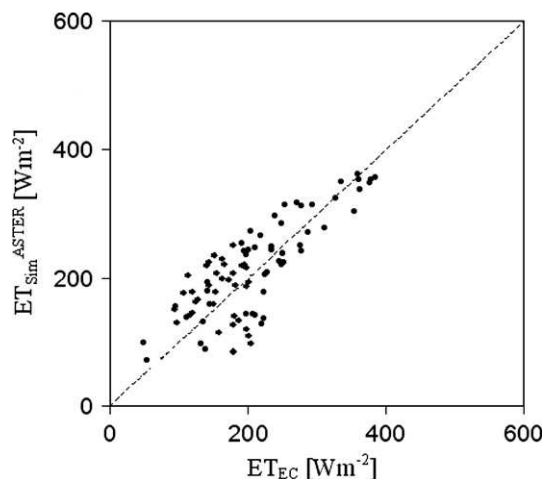


**Figure 10** Latent heat fluxes measured by the EC-system compared to latent heat fluxes calculated using both proposed formulations (for the evaporative fraction and for the available energy) with ASTER data.

directly into error in ET since it is estimated as the residual term of the energy balance equation. However, most approaches devoted to estimating ET from remote sensing data are susceptible to comparable errors.

## Discussion and conclusion

Sun synchronous optical remote sensing with high to moderate spatial resolution is often used for mapping instantaneous sensible and latent heat fluxes and evaporative fraction EF. The latter is often assumed to be constant throughout the day, enabling the estimation of daily evapotranspiration ET provided available energy AE is known. The daytime EF self preservation can be assumed under specific conditions, albeit sensitive to the time when EF is measured. The current study shows although EF remains fairly constant during daytime under dry conditions, but it depicts a concave up shape under wet conditions. Since the latter correspond to large evaporative fluxes, using a constant EF value throughout the day induces large errors in the calculation of daily ET.

Parameterizing the EF diurnal course from remotely sensed instantaneous estimates is twofold, with the goal of well reproducing a concave up shape under wet conditions while EF is self preserved under dry conditions. The first step integrates incoming solar radiation and relative humidity, two main factors for atmospheric demand given air temperature is indirectly considered through relative humidity whereas the impact of wind speed is minor. By first including these two atmospheric factors in the formulation, the EF diurnal course is well reproduced. The second step of the parameterization consists of incorporating land surface condition, since soil moisture and vegetation control the EF absolute value and day-to-day variations. Thus, the day to day variation as well as the spatial heterogeneities is taken into account by correcting EF from remotely sensed instantaneous ET.

This approach seems to include enough information on both atmospheric demand and land surface conditions to ac-

count for the diurnal and day-to-day fluctuations of EF — at least — under the prevailing conditions over the study site. However, this parameterization does not include the ET regulation by stomatal conductance. Thus, the relationship developed here is not universal, it needs to be assessed for more diverse ecosystems since plants differently respond to water stress whereas stomatal regulation depends on soil moisture. One might indeed expect that for trees for instance the physiological control on stem water storage or release would significantly affect the diurnal course of EF. Either the physiological control in our olive yard is mild in potential conditions, or the empirical equation used to derive the diurnal shape of EF takes into account the net effect of EF increase due to lower RH values and stomatal closure in the afternoon. Therefore, despite this empirical feature, the proposed approach is relevant for local applications. Indeed, its implementation over the considered Moroccan olive orchard decreases errors on water consumption estimates from 8% to 1% in relative, as compared to assuming EF is self preserved.

The next step towards estimating daily ET is deriving the AE diurnal course from a practical relationship. As for EF, a heuristic approach is used, which relies on variables either available from remote sensing data or fairly constant over areas up to several kilometers. Thus, the AE diurnal course is derived from remotely sensed AE when TERRA/ASTER overpasses, to be used along with meteorological observations for incoming shortwave and long wave irradiances. Though the proposed parameterization considers surface albedo is constant, the validation emphasizes good performances, with differences in AE lower than  $30 \text{ W m}^{-2}$ .

Once EF and AE are parameterized, the framework is applied to ASTER data, using a simple energy balance model (Santanello and Friedl, 2003; Lhomme and Elguero, 1999). The methodology is next applied to derive the ET diurnal course. After analyzing the footprint configuration, validation shows performances are comparable to other methods under similar conditions and data availabilities (Crow and Kustas, 2005). As for remote sensing approaches devoted to estimate daily ET, the proposed method is sensitive to errors on remotely sensed parameters. However, optimal use of in situ and remote sensing data allows a compromise between losing (respectively gaining) local (respectively regional) information. For operational applications, a temporal sampling of few days is needed. This is currently not possible with high spatial resolution TIR imagery, but could be in the near future. In the meanwhile, disaggregation of low spatial resolution thermal remote sensing data can be a possible solution; however this issue is still subject of ongoing investigations. Finally, it is of interest to mention that this proposed method has been recently applied to a mosaic of agricultural fields in northern Mexico to very encouraging results (Chehbouni et al., 2007c).

## Acknowledgments

This study has been funded by IRD, additional funding was provided by E.U. through the PLEIADES project. We are very grateful to all SUDMED research and technical staff for their help during the course of the experiment

## References

- Abrams, M., 2000. The advanced spaceborne thermal emission and reflection radiometer (ASTER): data products for the high spatial resolution imager on NASA's Terra platform. *International Journal of Remote Sensing* 21 (5), 847–859.
- Abrams, M., Hook, S., 2002. ASTER User Handbook Jet Propulsion Laboratory. Pasadena, California, 135 pp.
- Allen, R.G., 2000. Using the FAO-56 dual crop coefficient method over an irrigated region as part of an evapotranspiration intercomparison study. *Journal of Hydrology* 229, 27–41.
- Allen, R.G., Tasumi, M., Trezza, R., 2007. Satellite-based energy balance for mapping evapotranspiration with internalized calibration (METRIC) – model. *Journal of Irrigation and Drainage Engineering* 133 (4), 380–394.
- Asrar, G., Fuchs, M., Kanemasu, E.T., Hatfield, J.L., 1984. Estimating absorbed photosynthetic radiation and leaf area index from spectral reflectance in wheat. *Agronomy Journal* 76, 300–306.
- Baldocchi, D., 1997. Flux footprints within and over forest canopies. *Boundary-Layer Meteorology* 85, 273–292.
- Baldocchi, D.D., Xu, L.K., Kiang, N., 2004. How plant functional-type, weather, seasonal drought, and soil physical properties alter water and energy fluxes of an oak-grass savanna and an annual grassland. *Agricultural and Forest Meteorology* 123, 13–39.
- Bastiaanssen, W.G.M., Menenti, M., Feddes, R.A., Holtslag, A.A., 1998. A remote sensing surface energy balance algorithm for land (SEBAL): I. Formulation.. *Journal of Hydrology* 212–213 (1–4), 198–212.
- Bastiaanssen, W.G.M., Molden, D.J., Makin, I.W., 2000. Remote sensing for irrigated agriculture: examples from research and possible applications. *Agricultural Water Management* 46, 137–155.
- Batra, N., Islam, S., Venturini, V., Bisht, G., Jiang, L., 2006. Estimation and comparison of evapotranspiration from MODIS and AVHRR sensors for clear sky days over the Southern Great Plains. *Remote Sensing of Environment* 103, 1–15.
- Bisht, G., Venturini, V., Jiang, L., Islam, S., 2005. Estimation of the net radiation using MODIS (moderate resolution imaging spectroradiometer) data for clear sky days. *Remote Sensing of Environment* 97, 52–67.
- Braud, I., Dantas Antonino, A.C., Vauclin, M., Thony, J.L., Ruelle, P.A., 1995. Simple Soil Plant Atmosphere Transfer model (SiSPAT) development and field verification. *Journal of Hydrology* 166, 213–250.
- Brutsaert, W., 1982. *Evaporation into the Atmosphere*. Reidel, Dordrecht, 299 pp.
- Calvet, J.-C., Noilhan, J., Roujean, J.-L., Bessemoulin, P., Cabellguenne, M., Olioso, A., Wigneron, J.-P., 1998. An interactive vegetation SVAT model tested against data from six contrasting sites. *Agricultural and Forest Meteorology* 92, 73–95.
- Caparrini, F., Castelli, F., Entekhabi, D., 2003. Mapping of land-atmosphere heat fluxes and surface parameters with remote sensing data. *Boundary-Layer Meteorology* 107, 605–633.
- Caparrini, F., Castelli, F., Entekhabi, D., 2004. Variational estimation of soil and vegetation turbulent transfer and heat flux parameters from sequences of multisensor imagery. *Water Resources Research* 40, W12515. doi:10.1029/2004WR00335.
- Chandrapala, L., Wimalasuriya, M., 2003. Satellite measurements supplemented with meteorological data to operationally estimate evaporation in Sri Lanka. *Agricultural Water Management* 58, 89–107.
- Chaponnière, A., Boulet, G., Chehbouni, A., Aresmouk, M., 2007. Understanding hydrological processes with scarce data in a mountain environment. *Hydrological Processes*. doi:10.1002/hyp.677.
- Chebouni, A., Escadafal, R., Boulet, G., Duchemin, B., Simonneaux, V., Dedieu, G., Mougnot, B., Khabba, S., Kharrou, H., Merlin, O., Chaponnière, A., Ezzahar, J., Er-Raki, S., Hoedjes, J., Hadria, R., Abourida, H., Cheggour, A., Raïbi, F., Hanich, L., Guemouria, N., Chehbouni, A., Olioso, A., Jacob, F. and Sobrino, J., in press-a. The Use of Remotely Sensed data for Integrated Hydrological Modeling in Arid and Semi-Arid Regions: the SUDMED Program. *International Journal of Remote Sensing*.
- Chebouni, A., Ezzahar, J., Watts, C., Rodriguez, J.-C., Garatuza-Payan, J., in press-b. Estimating area-averaged surface fluxes over contrasted agricultural patchwork in a semi-arid region. In: Joachim Hill, Achim Röder (Eds.), *Advances in Remote Sensing and Geoinformation Processing for Land Degradation Assessment*, Taylor and Francis.
- Chebouni, A., Hoedjes, J., Rodriguez, J.-C., Watts, C., Garatuza, J., Jacob, F., Kerr, Y.H., 2007c. Using remotely sensed data to estimate area-averaged daily surface fluxes over a semi-arid mixed agricultural land. *Agricultural and Forest Meteorology*. doi:10.1111/j.1365-2486.2007.01466.
- Choudhury, B.J., Monteith, J.L., 1988. A four-layer model for the heat budget of homogeneous land surfaces. *Quarterly Journal of the Royal Meteorological Society* 114, 373–398.
- Cleugh, H.A., Leuning, R., Mu, Q., Running, S.W., 2007. Regional evaporation estimates from flux tower and MODIS satellite data. *Remote Sensing of Environment* 106, 285–304.
- Coudert, B., Ottlé, C., Boudevillain, B., Demarty, J., Guillevic, P., 2006. Contribution of Thermal Infrared remote sensing data in multiobjective calibration of a dual source SVAT model. *Journal of Hydrometeorology* 7 (3), 404–420.
- Crago, R.D., 1996. Conservation and variability of the evaporative fraction during daytime. *Journal of Hydrology* 180, 173–194.
- Crago, R.D., Brutsaert, W., 1996. Daytime evaporation and the self-preservation of the evaporative fraction and the Bowen ratio. *Journal of Hydrology* 178, 241–255.
- Crow, W.T., Kustas, W.P., 2005. Utility of assimilating surface radiometric temperature observations for evaporative fraction and heat transfer coefficient retrieval. *Boundary-Layer Meteorology* 115, 105–130.
- Duchemin, B., Hadria, R., Er-Raki, S., Boulet, G., Maisongrande, P., Chehbouni, A., Escadafal, R., Ezzahar, J., Hoedjes, J., Kharrou, M.H., Khabba, S., Mougnot, B., Olioso, A., Rodriguez, J.-C., Simonneaux, V., 2006. Monitoring wheat phenology and irrigation in Center of Morocco: on the use of relationship between evapotranspiration, crops coefficients, leaf area index and remotely-sensed vegetation indices. *Agricultural Water Management* 79, 1–27.
- Er-Raki, S., Chehbouni, A., Guemouria, N., Duchemin, B., Ezzahar, J., Hadria, R., 2007a. Combining FAO-56 model and ground-based remote sensing to estimate water consumptions of wheat crops in a semi-arid region. *Agricultural water management* 87, 41–54.
- Er-Raki, S., Chehbouni, A., Hoedjes, J., Ezzahar, J., Duchemin, B., Jacob, F., 2007b. Assimilation of ASTER based ET estimates in FAO 56 model over olive orchards in a semi-arid region. *Agricultural water management*. doi:10.1016/j.agwat.2007.10.01.
- Finn, D., Lamb, B., Leclerc, M.Y., Horst, T.W., 1996. Experimental evaluation of analytical and Lagrangian surface-layer footprint models. *Boundary-Layer Meteorology* 80, 283–308.
- French, A.N., Jacob, F., Anderson, M.C., Kustas, W.P., Timmermans, W., Gieske, A., Su, B., Su, H., McCabe, M.F., Li, F., Prueger, J., Brunsell, N., 2005. Surface energy fluxes with the Advanced Spaceborne Thermal Emission and Reflection radiometer (ASTER) at the Iowa 2002 SMACEX site (USA). *Remote Sensing of Environment* 99, 55–65.
- Fujisada, H., 1998. ASTER Level-1 data processing algorithm. *IEEE Transactions on Geoscience and Remote Sensing* 36, 1101–1112.
- Fujisada, H., Sakuma, F., Ono, A., Kudoh, M., 1998. Design and preflight performance of ASTER instrument protoflight model.



- IEEE Transactions on Geoscience and Remote Sensing 36 (4), 1152–1160.
- Gentine, P., Entekhabi, D., Chehbouni, A., Boulet, G., Duchemin, B., 2007. Analysis of evaporative fraction diurnal behaviour. *Agricultural and Forest Meteorology* 143, 13–29.
- Gillespie, A., Rokugawa, S., Matsunaga, T., Cothorn, J.S., Hook, S.J., Kahle, A.B., 1998. A temperature and emissivity separation algorithm for Advanced Spaceborne Thermal Emission and Reflection Radiometer (ASTER) images. *IEEE Transactions on Geoscience and Remote Sensing* 36 (4), 1113–1126.
- Glenn, E.P., Huete, A.R., Nagler, P.L., Hirschboeck, K.K., Brown, P., 2007. Integrating remote sensing and ground methods to estimate evapotranspiration. *Critical Reviews in Plant Sciences* 26 (3), 139–168.
- Gomez, M., Sobrino, J., Oliso, A., Jacob, F., 2005. Retrieval of evapotranspiration over the Alpillles test site using PolDER and thermal camera data. *Remote Sensing of Environment* 96, 399–408.
- Hoedjes, J.C.B., Zuurbier, R.M., Watts, C.J., 2002. Large aperture scintillometer used over a homogeneous irrigated area, partly affected by regional advection. *Boundary-Layer Meteorology* 105, 99–117.
- Hoedjes, J.C.B., Chehbouni, A., Ezzahar, J., Escadafal, R., De Bruin, H.A.R., 2007. Comparison of large aperture scintillometer and Eddy covariance measurements: can thermal infrared data be used to capture footprint induced differences? *Journal of Hydrometeorology* 8, 144–159.
- Horst, T.W., Weil, J.C., 1992. Footprint estimation for scalar flux measurements in the atmospheric surface layer. *Boundary-Layer Meteorology* 59, 279–296.
- Horst, T.W., Weil, J.C., 1994. How far is far enough?: The fetch requirements for micrometeorological measurement of surface fluxes. *Journal of Oceanic and Atmospheric Technology* 11, 1018–1025.
- Jackson, R.D., Reginato, R.J., Idso, S.B., 1977. Wheat canopy temperature: a practical tool for evaluating water requirements. *Water Resources Research* 13, 651–656.
- Jackson, R.D., Hatfield, J.L., Reginato, R.J., Idso, S.B., Pinter Jr., P.J., 1983. Estimation of daily evapotranspiration from one time-of-day measurements. *Agricultural Water Management* 7, 351–362.
- Jacob, F., Weiss, M., Oliso, A., French, A., 2002. Assessing the narrowband to broadband conversion to estimate visible, near infrared and shortwave apparent albedo from airborne PolDER data. *Agronomie: Agriculture and Environment* 22, 537–546.
- Jacob, F., Petitcolin, F., Schmugge, T., Vermote, E., French, A., Ogawa, K., 2004. Comparison of land surface emissivity and radiometric temperature derived from MODIS and ASTER sensors. *Remote Sensing of Environment* 90, 137–152.
- Jacob, F., Oliso, A., 2005. Derivation of diurnal courses of albedo and reflected solar irradiance from airborne POLDER data acquired near solar noon. *Journal of Geophysical Research* 110, D10104. doi:10.1029/2004JD00488.
- Jacob, F., Schmugge, T., Oliso, A., French, A., Courault, D., Ogawa, K., Petitcolin, F., Chehbouni, G., Pinheiro, A., Privette, J., in press. Modeling and inversion in thermal infrared remote sensing over vegetated land surfaces. In: *Advances in Land Remote Sensing: System, Modeling, Inversion and Application* (S. Liang Ed.), Springer.
- Leclerc, M.Y., Shen, S., Lamb, B., 1997. Observations and large-eddy simulation modeling of footprints in the lower convective boundary layer. *Journal of Geophysical Research* 102, 9323–9334.
- Lhomme, J.-P., Monteny, B., Amadou, M., 1994. Estimating sensible heat flux from radiometric temperature over sparse millet. *Agricultural and Forest Meteorology* 68, 77–91.
- Lhomme, J.-P., Elguero, E., 1999. Examination of evaporative fraction diurnal behaviour using a soil-vegetation model coupled with a mixed-layer model. *Hydrology and Earth System Sciences* 3 (2), 259–270.
- Li, S.-G., Eugster, W., Asanuma, J., Kotani, A., Davaa, G., Oyunbaatar, D., Sugita, M., 2006. Energy partitioning and its biophysical controls above a grazing steppe in central Mongolia. *Agricultural and Forest Meteorology* 137 (1–2), 89–106.
- Liu, Y., Hiyama, T., Yamaguchi, Y., 2006. Scaling of land surface temperature using satellite data: a case examination on ASTER and MODIS products over a heterogeneous terrain area. *Remote Sensing of Environment* 105, 115–128.
- Mahfouf, J.F., Manzi, A.O., Noilhan, J., Giordani, H., Déqué, M., 1995. The land surface scheme ISBA within the Météo-France climate model ARPEGE. Part I. Implementation and preliminary results. *Journal of Climate* 8, 2039–2057.
- Mu, Q., Heinsch, F.A., Zhao, M., Running, S.W., 2007. Development of a global evapotranspiration algorithm based on MODIS and global meteorology data. *Remote Sensing of Environment* 111 (4), 519–536.
- Nichols, W.E., Cuenca, R.H., 1993. Evaluation of the evaporative fraction for parameterization of the surface, energy-balance. *Water Resources Research* 29, 3681–3690.
- Norman, J.M., Anderson, M.C., Kustas, W.P., French, A.N., Mecikalski, J., Torn, R., Diak, G.R., Schmugge, T.J., Tanner, B.C.W., 2003. Remote sensing of surface energy fluxes at 10<sup>1</sup>-m pixel resolutions. *Water Resources Research* 39 (8), 1221. doi:10.1029/2002WR00177.
- Ogawa, K., Schmugge, T., Jacob, F., French, A., 2003. Estimation of land surface window (8–12 μm) emissivity from multi-spectral thermal infrared remote sensing—A case study in a part of Sahara Desert. *Geophysical Research Letters* 30, 1067–1071.
- Ohmura, A., Wild, M., 2002. Is the hydrological cycle accelerating? *Science* 298, 1345–1346.
- Oliso, A., Carlson, T.N., Brisson, N., 1996. Simulation of diurnal transpiration and photo-synthesis of a water stressed soybean crop. *Agricultural and Forest Meteorology* 81, 41–59.
- Oliso, A., Inoue, Y., Ortega-Farías, S., Demarty, J., Wigneron, J.-P., Braud, I., Jacob, F., Lecharpentier, P., Ottlé, C., Calvet, J.-C., Brisson, N., 2005. Future directions for advanced evapotranspiration modeling: assimilation of remote sensing data into crop simulation models and SVAT models. *Irrigation and Drainage Systems* 19 (3–4), 355–376.
- Porporato, A., Daly, E., Rodriguez-Iturbe, I., 2004. Soil water balance and ecosystem response to climate change. *American Naturalist* 164, 625–632.
- Rannik, Ü., Aubinet, M., Kurbanmuradov, O., Sabelfeld, K.K., Markkanen, T., Vesala, T., 2000. Footprint analysis for measurements over a heterogeneous forest. *Boundary-Layer Meteorology* 97, 137–166.
- Roerink, G.J., Su, Z., Menenti, M., 2000. S-SEBI: a simple remote sensing algorithm to estimate the surface energy balance. *Physics and Chemistry of the Earth (B)* 25 (2), 147–157.
- Santanello, J.A., Friedl, M.A., 2003. Diurnal covariation in soil heat flux and net radiation. *Journal of Applied Meteorology* 42, 851–862.
- Schmugge, T., Hook, S.J., Coll, C., 1998. Recovering surface temperature and emissivity from thermal infrared multispectral data. *Remote Sensing of Environment* 65 (2), 121–131.
- Schuepp, P.H., Leclerc, M.Y., MacPherson, J.L., Desjardins, R.L., 1990. Footprint prediction of scalar fluxes from analytical solutions of the diffusion equation. *Boundary-Layer Meteorology* 50, 355–373.
- Schuurmans, J.M., Troch, P.A., Veldhuizen, A.A., Bastiaanssen, W.G.M., Bierkens, M.F.P., 2003. Assimilation of remotely sensed latent heat flux in a distributed hydrological model. *Advances in Water Resources* 26, 151–159.
- Seguin, B., Assad, E., Freteaud, P., Imbernon, J.-P., Kerr, Y.H., Lagouarde, J.-P., 1989. Use of meteorological satellites for



- 935 water balance monitoring in Sahelian regions. *International*  
936 *Journal of Remote Sensing* 10, 1001–1017.
- 937 Shuttleworth, W.J., Gurney, R.J., Hsu, A.Y., Ormsby, J.P.,  
938 1989FIFE: The Variation in Energy Partition at Surface Flux  
939 Sites, vol. 186. IAHS Publication, pp. 67–74.
- 940 Shuttleworth, W.J., Gurney, R.J., 1990. The theoretical relation-  
941 ship between foliage temperature and canopy resistance in  
942 sparse crops. *Quarterly Journal of the Royal Meteorological*  
943 *Society* 116, 497–519.
- 944 Sugita, M., Brutsaert, W., 1991. Daily evaporation over a region  
945 from lower boundary layer profiles. *Water Resources Research*  
946 27, 747–752.
- 947 Suleiman, A., Crago, R.D., 2004. Hourly and daytime evapotrans-  
948 piration from grassland using radiometric surface temperatures.  
949 *Agronomy Journal* 96, 384–390.
- 950 Twine, T.E., Kustas, W.P., Norman, J.M., Cook, D.R., Houser, P.R.,  
951 Meyers, T.P., Prueger, J.H., Starks, P.J., Wesely, M.L., 2000.  
952 Correcting Eddy-covariance flux underestimates over a grass-  
953 land. *Agricultural and Forest Meteorology* 103, 279–300.
- 954 Thome, K., Palluconi, F., Takashima, T., Masuda, K., 1998.  
955 Atmospheric correction of ASTER. *IEEE Transactions on Geosci-*  
956 *ence and Remote Sensing* 36, 1199–1211.
- 957 Van den Hurk, B.J.J.M., Bastiaanssen, W.G.M., Pelgrum, H., Van  
958 Meijgaard, E., 1997. A new methodology for initialization of soil  
959 moisture fields in numerical weather prediction models using  
960 METEOSAT and NOAA data. *Journal of Applied Meteorology* 36,  
961 1271–1283.
- 962 Van Dijk, A., Moene, A.F. De Bruin, H.A.R., 2004. The principles of  
963 surface flux physics: theory, practice and description of the  
964 ECPACK library. Internal Report 2004/1, Meteorology and Air  
Quality Group, Wageningen University, Wageningen, The Neth-  
erlands, 99 pp.
- Wang, K., Li, Z., Cribb, M., 2006. Estimation of evaporative  
fraction from a combination of day and night land surface  
temperatures and NDVI: a new method to determine the  
Priestley-Taylor parameter. *Remote Sensing of Environment*  
102, 293–305.
- Weiss, M., Jacob, F., Baret, F., Pragnère, A., Bruchou, C., Leroy,  
M., Hauteceur, O., Prévot, L., Bruguier, N., 2002. Evaluation  
of kernel-driven BRDF models for the normalization of Alpilles/  
ReSeDA POLDER data. *Agronomie* 22, 531–536.
- Wild, M., Ohmura, A., Gilgen, H., Rosenfeld, D., 2004. On the  
consistency of trends in radiation and temperature records and  
implications for the global hydrological cycle. *Geophysical*  
*Research Letters* 31, L11201. doi:10.1029/2003GL01918.
- Williams, D.G., Cable, W., Hultine, K., Hoedjes, J.C.B., Yezpe,  
E.A., Simonneaux, V., Er-Raki, S., Boulet, G., De Bruin, H.A.R.,  
Chehbouni, A., Hartogensis, O.K., Timouk, F., 2004. Evapo-  
transpiration components determined by stable isotope, sap  
flow and eddy covariance techniques. *Agricultural and Forest*  
*Meteorology* 125, 241–258.
- Yang, F., White, M.A., Michaelis, A.R., Ichii, K., Hashimoto, H.,  
Votava, P., Zhu, A-X., Nemani, R.R., 2006. Prediction of  
continental-scale evapotranspiration by combining MODIS and  
AmeriFlux data through support vector machine. *IEEE Trans-*  
*actions on Geoscience and Remote Sensing* 44 (11), 3452–  
3461.
- Zhang, L., Lemeur, R., 1995. Evaluation of daily evapotranspiration  
estimates from instantaneous measurements. *Agricultural and*  
*Forest Meteorology* 74, 139–154.